of E_{abs} suggest that models that assume internal mixtures in a core-shell configuration, or scale the absorption (or forcing) by externally mixed BC particles, can substantially overestimate the atmospheric warming by BC, potentially by up to a factor of 2 (*4*, *5*). The climate benefits of BC mitigation (*3*) would similarly be overestimated. This would be true even for models that specifically track the mixing state of BC particles as they evolve in time (*25*). It is possible that non–fossil-derived BC (such as emitted from biomass burning) may exist with a considerably different internal morphology or amounts of BrC as compared with the ambient particles observed in this study, and thus different observable E_{abs} values. Models may ultimately need to treat BC from fossil-fuel combustion differently than BC from biomass burning, although this awaits validation through further measurements of wavelength-dependent E_{abs} for atmospheric particles in a variety of locations around the world. The contrast between our ambient observations and model formulations highlights the still incomplete understanding of radiative forcing by atmospheric BC with respect to particle-mixing state. Additional challenges include the quantification of BC emission inventories, wet-deposition removal rates, and the specification of the spatial and temporal distributions of BC (particularly the altitudinal profile) (*26*).

References and Notes

1. V. Ramanathan, G. Carmichael, *Nat. Geosci.* **1**, 221 (2008).
2. A. P. Grieshop, C. C. O. Reynolds, M. Kandlikar, H. Dowlatabadi, *Nat. Geosci.* **2**, 533 (2009).
3. D. Shindell *et al.*, *Science* **335**, 183 (2012).
4. S. H. Chung, J. H. Seinfeld, *J. Geophys. Res.* **110**, (D11), D11102 (2005).
5. M. Z. Jacobson, *Nature* **409**, 695 (2001).
6. G. Myhre, *Science* **325**, 187 (2009).
7. T. C. Bond, G. Habib, R. W. Bergstrom, *J. Geophys. Res.* **111**, (D20), D20211 (2006).
8. J. Hansen *et al.*, *Clim. Dyn.* **29**, 661 (2007).
9. A. Knox *et al.*, *Aerosol Sci. Technol.* **43**, 522 (2009).
10. C. Doran, *Atmos. Chem. Phys.* **7**, 2197 (2007).
11. S. J. Ghan, S. E. Schwartz, *Bull. Am. Meteorol. Soc.* **88**, 1059 (2007).
12. Materials and methods are available as supplementary materials on *Science* Online.
13. M. O. Andreae, A. Gelencser, *Atmos. Chem. Phys.* **6**, 3131 (2006).
14. T. B. Onasch *et al.*, *Aerosol Sci. Technol.* **46**, 804 (2012).
15. D. A. Lack, C. D. Cappa, *Atmos. Chem. Phys.* **10**, 4207 (2010).
16. K. Adachi, S. H. Chung, P. R. Buseck, *J. Geophys. Res.* **115**, (D15), D15206 (2010).
17. K. S. Johnson *et al.*, *Atmos. Chem. Phys.* **5**, 3033 (2005).
18. J. Li, J. R. Anderson, P. R. Buseck, *J. Geophys. Res.* **108**, (D6), 4189 (2003).
19. E. S. Cross *et al.*, *Aerosol Sci. Technol.* **44**, 592 (2010).
20. M. Schnaiter *et al.*, *J. Geophys. Res.* **110**, (D19), D19204 (2005).
21. J. C. Barnard, R. Volkamer, E. I. Kassianov, *Atmos. Chem. Phys.* **8**, 6665 (2008).
22. R. R. Dickerson *et al.*, *Science* **278**, 827 (1997).
23. M. Z. Jacobson, *J. Geophys. Res.* **104**, (D3), 3527 (1999).
24. D. T. Shindell *et al.*, *Science* **326**, 716 (2009).
25. R. A. Zaveri, J. C. Barnard, R. C. Easter, N. Riemer, M. West, *J. Geophys. Res.* **115**, (D17), D17210 (2010).
26. D. Koch *et al.*, *Atmos. Chem. Phys.* **9**, 9001 (2009).

Acknowledgments: The authors thank the crew of the R/V *Atlantis*, the support at American River College and Cambustion for loan of the centrifugal particle mass analyzer (CPMA). This work was supported by the NOAA Climate Program Office (NA09OAR4310124 and NA09OAR4310125), U.S. Environmental Protection Agency (RD834558), NSF Atmospheric Chemistry, California Air Resources Board, U.S. Department of Energy (DOE) Atmospheric System Research (ASR) program and DOE Atmospheric Radiation Measurement (ARM) Climate Research Facility, the Canadian Federal Government (PERD Project C12.007), and the Natural Sciences and Engineering Research Council of Canada.

Supplementary Materials

www.sciencemag.org/cgi/content/full/337/6098/1078/DC1
Materials and Methods
Figs. S1 to S19
References

17 April 2012; accepted 3 July 2012
10.1126/science.1223447

A Gain-of-Function Polymorphism Controlling Complex Traits and Fitness in Nature

Kasavajhala V. S. K. Prasad,[1]* Bao-Hua Song,[1]* Carrie Olson-Manning,[1]* Jill T. Anderson,[1] Cheng-Ruei Lee,[1] M. Eric Schranz,[1]† Aaron J. Windsor,[1]‡ Maria J. Clauss,[2] Antonio J. Manzaneda,[1]§ Ibtehaj Naqvi,[1]|| Michael Reichelt,[2] Jonathan Gershenzon,[2] Sanjeewa G. Rupasinghe,[3]¶ Mary A. Schuler,[3] Thomas Mitchell-Olds[1]#

Identification of the causal genes that control complex trait variation remains challenging, limiting our appreciation of the evolutionary processes that influence polymorphisms in nature. We cloned a quantitative trait locus that controls plant defensive chemistry, damage by insect herbivores, survival, and reproduction in the natural environments where this polymorphism evolved. These ecological effects are driven by duplications in the *BCMA* (branched-chain methionine allocation) loci controlling this variation and by two selectively favored amino acid changes in the glucosinolate-biosynthetic cytochrome P450 proteins that they encode. These changes cause a gain of novel enzyme function, modulated by allelic differences in catalytic rate and gene copy number. Ecological interactions in diverse environments likely contribute to the widespread polymorphism of this biochemical function.

Few studies have identified the genes that underlie complex trait variation in nature and the evolutionary processes that influence these polymorphisms. Most such work has focused on loss-of-function mutations that lead to adaptive phenotypes (*1*), likely because novel gain-of-function changes occur infrequently and require persistent natural selection to be maintained in populations (*2*). Nonetheless, new functional mechanisms are crucially important for adaptive evolution (*3*). To understand the adaptive consequences of complex trait variation, we must establish a direct relationship between genetic polymorphisms and phenotypic traits, and investigate the fitness consequences of this variation in natural environments (*1*).

Glucosinolates are biologically active secondary compounds (fig. S1) found in *Arabidopsis* and its relatives (*4*) that are important in many aspects of plant defense, influencing oviposition and feeding by insect herbivores (*5*), defense against microbial pathogens (*6*), and composition of associated microbial communities (*7*). Typically, generalist insects are sensitive to glucosinolate-based plant defenses, whereas specialists may be able to cope with these compounds, which may serve as oviposition cues and feeding stimulants (*5*).

The ecological model plant *Boechera stricta* (Brassicaceae) is a native, short-lived perennial with a close phylogenetic relationship to *Arabidopsis* (*8*), often found in undisturbed habitats where current environments are similar to historical conditions that have existed for ~3000 years (*9*). In field populations near Lost Trail Pass in Montana and Crested Butte in Colorado, we measured natural selection on foliar damage from herbivores using local genotypes. We mapped a quantitative trait locus (QTL) in *B. stricta* that contributes to insect resistance and controls allocation to glucosinolates derived from branched-chain amino acids or methionine [the *BCMA* (branched-chain methionine allocation) locus] (*10*). Although most Brassicaceae synthesize glucosinolates from

[1]Department of Biology, Institute for Genome Sciences and Policy, Duke University, Durham, NC 27708, USA. [2]Max Planck Institute for Chemical Ecology, D-07745 Jena, Germany. [3]Department of Cell and Developmental Biology, University of Illinois at Urbana-Champaign, Urbana, IL 61801, USA.

*These authors contributed equally to this work.
†Present address: Biosystematics Group, Wageningen University, 6708 PB Wageningen, Netherlands.
‡Present address: Bayer CropScience N.V., 9052 Ghent, Belgium.
§Present address: Departmento de Biologia Animal, Biologia Vegetal y Ecologia, Area de Ecologia, Universidad de Jaen, 23071 Jaen, Spain.
||Present address: Duke University School of Medicine, Durham, NC 27710, USA.
¶Present address: Pfizer Inc., MS 8118A-2053, Eastern Point Road, Groton, CT 06340, USA.
#To whom correspondence should be addressed. E-mail: tmo1@duke.edu

methionine or tryptophan precursors, among the genera closely related to *Arabidopsis*, only *Boechera* produces glucosinolates from branched-chain amino acids, specifically valine or isoleucine (*11*). We refer to these two categories of methionine-derived and branched-chain glucosinolates as Met-GS and BC-GS, respectively.

We examined variation in *B. stricta* for three herbivory-related traits: leaf damage by herbivores, total glucosinolates, and BC ratio (i.e., the proportion of aliphatic glucosinolates derived from valine or isoleucine) in nine natural populations in Idaho and Montana, and found significant genetic variation for all traits (table S1) (*12*). Levels of herbivore damage (percentage of leaf area removed) and total quantity of foliar glucosinolates showed genetic variation (Fig. 1 and table S1; $P = 0.0355$ for herbivore damage among families, other $P < 0.0001$) and continuous phenotypic distributions typical of complex traits. In contrast, we found a discontinuous distribution in the proportion of aliphatic BC-GS versus Met-GS (Fig. 1), which corresponds to the *BCMA* QTL (*12*, *13*). The parental genotypes examined here have glucosinolate phenotypes that are representative of other plants in these populations (*12*).

We quantified the ecological effects of this variation by measuring late-season foliar glucosinolates in 1030 F_6 near-isogenic line (NIL) plants in the Montana (MT) and Colorado (CO) field sites. Segregation of the *BCMA* locus predicted the BC ratio in both environments ($P < 10^{-199}$; table S2) and both were significant predictors of insect damage ($P < 0.008$; table S3). Early-season herbivory showed significant effects of *BCMA* in Montana ($P < 10^{-6}$; table S4) but not in Colorado. However, the *BCMA* × site interaction for herbivore damage was not significant early in the season ($P = 0.092$; table S4) or for maximum damage on plants that survived through the summer (table S3). The quantitative level of leaf damage was a significant predictor of mortality in both Montana and Colorado ($P = 0.0017$; table S5), with no hint of heterogeneous selection gradients among sites (damage × site interaction, $P = 0.48$). Combining the observed levels of damage and estimates of natural selection (Fig. 2 and table S4), we calculate that the *BCMA-MT* homozygote had 1.3% higher fitness than the *BCMA-CO* genotype (*12*).

We compared herbivore damage and fecundity on 1435 recombinant inbred line (RIL) plants, in 2009 in Montana and in 2010 in Colorado. Mean herbivore damage was higher in Colorado (64.2 ± 5.8%) than in Montana (10.3 ± 1.9%). *BCMA* genotype predicted herbivore damage in Montana, with the *BCMA-CO* homozygote showing higher damage than the native *BCMA-MT* genotype (14.0 and 9.0%, respectively, $P < 0.0001$; table S6). In contrast, *BCMA* genotypes showed no significant difference in damage levels in Colorado ($P = 0.63$), perhaps because herbivores in Colorado are resistant to these compounds, or because chemical defenses were overwhelmed by high levels of herbivory. This *BCMA* × site interaction for herbivore damage was significant ($P = 0.019$; table S6). In addition, herbivore damage was a significant predictor of fecundity in Montana (Fig. 2, $P < 0.013$; table S7) but not in Colorado ($P = 0.72$), with a significant *BCMA* × site interaction for probability of fruiting ($P = 0.05$; table S8). In Montana the local allele enhances the probability of fruiting by 132% relative to the Colorado allele (*12*); however, there is no effect of allelic variation in Colorado. Combining observed levels of damage and estimates of natural selection, we calculate that the *BCMA-MT* homozygote had 12% higher fecundity in Montana than did the Colorado homozygote (Fig. 2 and table S6) (*12*). Such large fitness differences may explain why many populations are nearly fixed for *BCMA* (Fig. 1B). Overall, the protective effect of *BCMA* against herbivory appears to differ between sites (table S6), whereas substantial fitness reduction due to leaf damage is commonly observed across sites and years (Fig. 2).

To control for the effects on fitness caused by linked genes, as well as other selective factors that might be correlated with herbivore damage, we planted 1539 F_6 NIL plants where each was assigned to an undamaged control group or to artificial herbivory (removal of ~33% of each leaf) (*12*). On average, a loss of 1% of leaf area caused a 1.2% reduction in survival (Fig. 2), with significantly elevated mortality in the herbivory treatment ($P < 0.0001$; table S9).

In *Arabidopsis thaliana*, the *CYP79F* locus encodes the first step of the core Met-GS pathway (*14*, *15*) and *CYP83A* encodes the second step (*16*, *17*). We sequenced bacterial artificial chromosomes (BACs) from both genotypes that gave rise to the RIL and NIL populations, and identified nine markers within the 1-cM interval

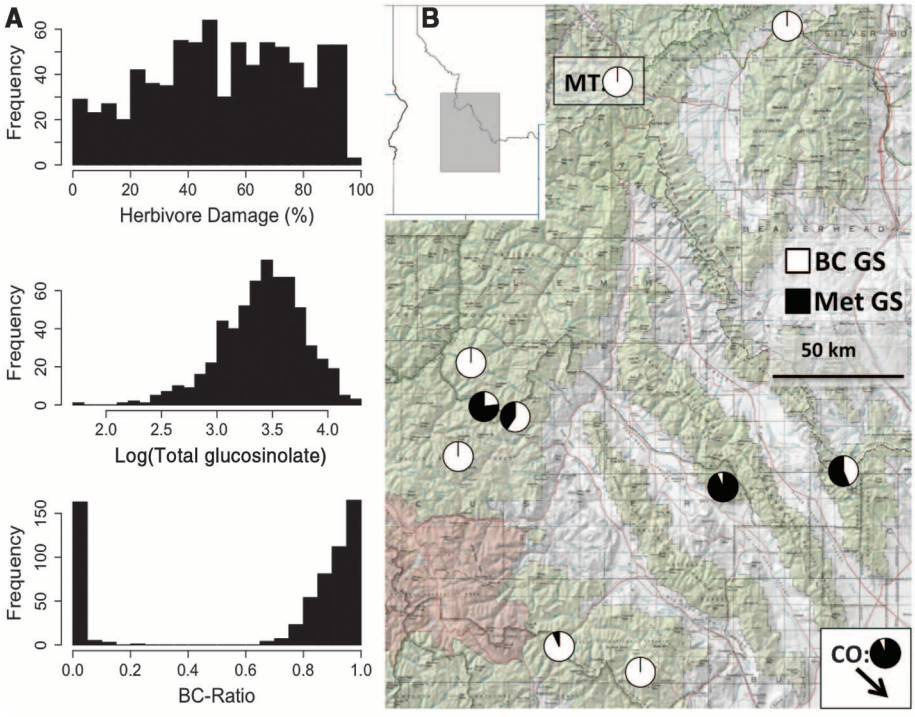

Fig. 1. (**A**) Histograms show percent leaf area removed by the generalist herbivore *Trichoplusia ni*, total quantity of glucosinolates, and proportion of aliphatic glucosinolates from branched-chain amino acid precursors (BC-GS). Greenhouse-grown plants were descended from nine *B. stricta* populations. (**B**) Map showing the proportion of genotypes in each population that produce predominantly BC-GS (white) or Met-GS (black). Parental populations of the crossing experiment are boxed.

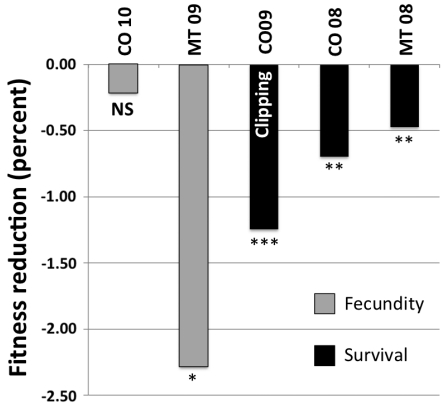

Fig. 2. Fitness reductions under field conditions associated with 1% loss of leaf area by herbivory. Bars indicate reduction in components of fitness due to fecundity (gray) and survival (black) in 2008, 2009, and 2010 in Colorado and Montana. NIL plants in the clipping experiment were randomly assigned to artificial herbivory or control treatments. *$P < 0.05$, **$P < 0.01$, ***$P < 0.001$; NS, not significant.

containing the *BCMA* QTL. These included sequences orthologous to *CYP79F* and *CYP83A*. *CYP83A* is 0.33 cM from the peak lod score (logarithm of the odds ratio for linkage) for the *BCMA* QTL (fig. S2 and table S10), whereas the *CYP79* polymorphism has a peak lod score of 365.3, with 10-lod confidence interval < 0.1 cM wide (fig. S2 and table S10).

We created transgenic *Arabidopsis* plants for each locus and allele of the *CYP79* gene family from *Boechera* (*12*). Phenotypes of the transgenic plants show that the *BCMA* biochemical polymorphism is controlled by these *CYP79* loci, hence *BCMA* is a gene family with three expressed copies (fig. S3). These enzymes convert amino acids to their corresponding oximes in the first step of glucosinolate biosynthesis (*15*). *BCMA2* is syntenic with the *CYP79F1* region in *A. thaliana* but is not linked to the *BCMA* QTL that controls the BC ratio. *BCMA3* and *BCMA1* are tightly linked at the LOD peak of the *BCMA* QTL, with *BCMA3* present in both parental genotypes, whereas *BCMA1* is only present in the Montana genotype.

We expressed these *BCMA* sequences and controls in 130 independent *Arabidopsis* transformants to control for position effects and number of insertions. We found significant differences in foliar glucosinolates derived from methionine, valine, or isoleucine in transgenic plants ($P < 10^{-45}$; Fig. 3A, fig. S4, and table S11). *BCMA1-MT* transgenics showed increased production of isoleucine-derived glucosinolates ($P < 0.04$), and both *BCMA3* alleles caused increased production of valine-derived glucosinolates ($P = 0.034$ and $P = 0.0001$ for *BCMA-CO* and *BCMA-MT*, respectively) relative to controls. In addition, *BCMA1-MT* and both *BCMA2* alleles caused modest increases in methionine-derived glucosinolates ($P = 0.028$ to $P = 0.002$).

We compared *BCMA3-MT* and *BCMA3-CO* transgenics and found no significant difference for total concentration of aliphatic glucosinolates ($P > 0.05$; table S11). However, the *BCMA3-MT* allele produced higher levels of valine glucosinolates than did the *BCMA3-CO* allele (factor of 3.5; $P = 0.0002$). The *CO* allele differs from *BCMA3-MT* by an amino acid substitution in the substrate-binding region, which may be responsible for this reduced concentration of valine glucosinolates in transgenic plants. Finally, allele-specific expression to test for cis-regulatory variation found no significant differences in gene expression (*12*).

Heterologous expression in *Escherichia coli* also indicated that the enzymes encoded by *BCMA1* and *BCMA3*, but not *BCMA2*, have acquired catalytic activity toward branched-chain amino acid precursors (the "BC-AA clade," which includes an orthologous sequence from *B. retrofracta*, which also produces BC-GS) (*11*). Comparing the rate of nonsynonymous versus synonymous substitution with maximum likelihood in PAML (*18*) indicated that the branch leading to the BC-AA clade (branch F in fig. S5) has undergone accelerated biochemical evolution ($P = 0.036$; table S12). In addition, two amino acid sites (134 and 536) in the BC-AA clade also showed rapid evolution (table S13).

The BCMA1-MT enzyme has evolved elevated activity toward isoleucine (Fig. 3B and table S14). For valine, we found significant catalytic activity for BCMA1 and BCMA3 and a modest increase for BCMA2. Although transgenic analysis showed that the *BCMA3-MT* allele produced higher levels of valine glucosinolates than the *BCMA3-CO* allele, heterologous expression did not detect a significant difference in the rate of valine catalysis between these *BCMA3* alleles ($t = 1.09$, df = 6, $P = 0.32$). This may reflect differences in experimental variation between transgenic plants and in vitro assays, glucosinolate turnover in vivo, or enzyme function in vitro versus in vivo. Finally, we mutated Gly^{134} and Pro^{536} in BCMA2 (to BCMA1/3 residues Leu and Lys, respectively; henceforth G134L and P536K) to assay their effect on catalytic activity on valine and isoleucine. Either mutation, or both together, caused increased activity toward valine ($P = 0.0361$ to $P = 0.0004$; Fig. 3B and table S14).

The tertiary structures of eukaryotic cytochrome P450 proteins are highly conserved despite substantial divergence in their primary structures (*19*, *20*). We predicted the structure

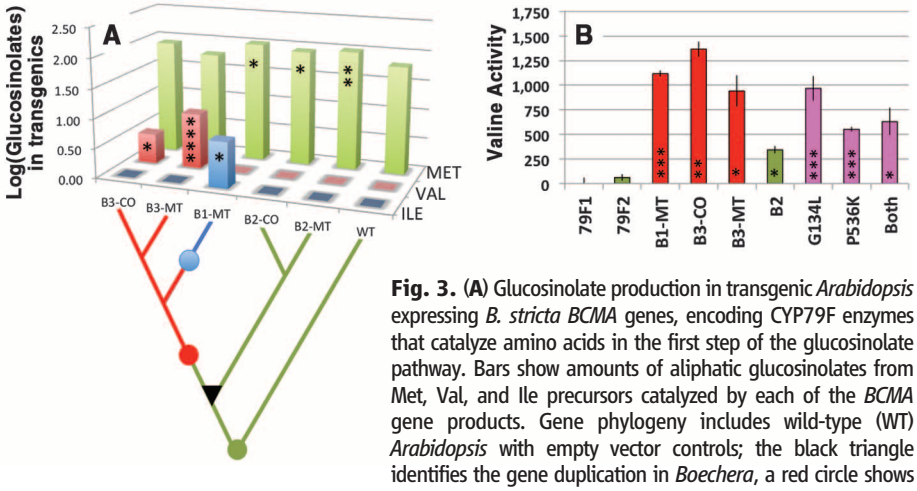

Fig. 3. (**A**) Glucosinolate production in transgenic *Arabidopsis* expressing *B. stricta BCMA* genes, encoding CYP79F enzymes that catalyze amino acids in the first step of the glucosinolate pathway. Bars show amounts of aliphatic glucosinolates from Met, Val, and Ile precursors catalyzed by each of the *BCMA* gene products. Gene phylogeny includes wild-type (WT) *Arabidopsis* with empty vector controls; the black triangle identifies the gene duplication in *Boechera*, a red circle shows the origin of branched-chain amino acid catalysis, and a blue circle indicates elevated Ile activity. Abbreviations: B1, *BCMA1*; B2, *BCMA2*; B3, *BCMA3*, with alleles from Colorado (CO) or Montana (MT). $N = 130$ independent transgenic lines. (**B**) In vitro enzyme activity levels (nmol of product per nmol of enzyme per minute) relative to controls; error bars denote SE. Labels indicate CYP79F enzymes from *Arabidopsis* and BCMA1, BCMA2, and BCMA3 from *Boechera*, with alleles from Colorado or Montana. BCMA2 alleles encode identical proteins, so one allele was assayed. BCMA2 (green) retains the ancestral MET activity and was engineered to change G134L, P536K, or both (pink). $*P < 0.05$, $**P < 0.01$, $***P < 0.001$.

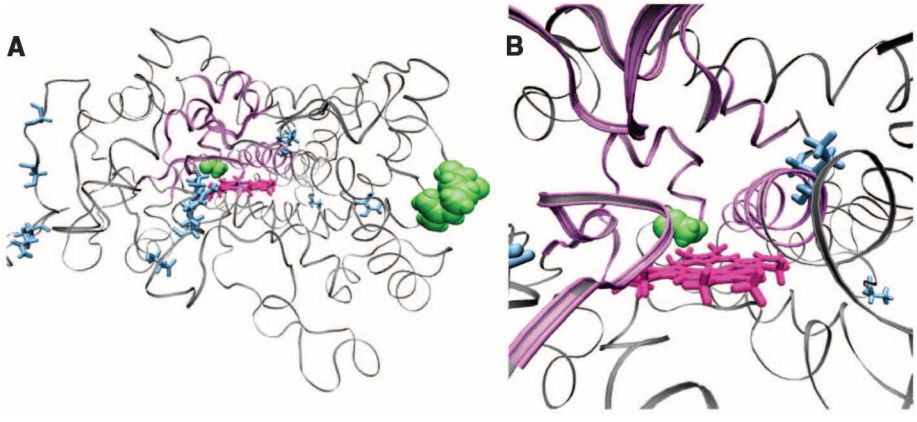

Fig. 4. (**A**) Homology model of BCMA2 with the substrate-binding cleft above the heme group (magenta) with putative substrate recognition regions in purple. Amino acid changes G134L and P536K (green) show statistical evidence for accelerated protein evolution and alter catalytic function when changed by site-directed mutagenesis. Other mutations with statistical evidence of accelerated evolution (in blue) are not addressed in this study. The location of amino acid 529, which aligns with the last resolved residue in the CYP1A2 crystal structure, is colored because subsequent amino acids 530 to 540 cannot be accurately modeled. (**B**) Close-up view of substrate-binding cleft with mutation G134L residing just above the heme.

of BCMA2 (Fig. 4) and visualized the locations of variations in the BCMA1 and BCMA3 proteins that might explain their altered catalytic functions. G134L, one of the two residues showing evidence for accelerated molecular evolution, occurs in substrate recognition site SRS1 near the heme (Fig. 4) and is predicted to alter the catalytic site space in the region closest to the heme. The other, P536K, occurs five amino acids upstream from their C termini and is predicted to alter electrostatic interactions of this flexible tail region. Mapping of the two positions varying between the BCMA3-MT and BCMA3-CO alleles indicates that $Val^{148} \rightarrow$ Leu occurs in a region potentially affecting interactions with electron transfer partners, and that $Met^{268} \rightarrow$ Val occurs in a SRS3 region predicted to affect the volume of the upper catalytic site and/or substrate access (fig. S6). However, determining the biochemical effects of these changes is beyond the scope of this study.

We have shown how the *BCMA* QTL affects plant chemistry and insect resistance, and thus fitness, in a quantitative manner. In *Boechera*, the *BCMA2* locus retains ancestral activity and synteny, whereas *BCMA1* and *BCMA3* have evolved novel catalytic activity. The resulting polymorphic Met-GS and BC-GS show heterogeneous effects on host plant resistance against diverse enemies across a range of environments. In the Montana population, homozygotes at *BCMA* produce BC-GS and show greater resistance to damage by a diverse community of herbivores (tables S4 and S6). Further evidence that these compounds have environment-dependent consequences comes from transgenic *Arabidopsis*, where BC-GS cause increased resistance to the pathogen *Erwinia carotovora* (*6*), and from other herbivores, where BC-GS cause increased susceptibility to *Trichoplusia ni* (*10*). However, *BCMA* has no effect on insect damage in Colorado (tables S4 and S6), where other loci control resistance (table S6). On the basis of this study, we conclude that heterogeneous responses to diverse biotic interactions in the context of selection by herbivores likely contribute to the genetic diversity of *BCMA*.

References and Notes

1. R. D. Barrett, H. E. Hoekstra, *Nat. Rev. Genet.* **12**, 767 (2011).
2. R. L. Rogers, D. L. Hartl, *Mol. Biol. Evol.* **29**, 517 (2012).
3. D. J. Futuyma, A. A. Agrawal, *Proc. Natl. Acad. Sci. U.S.A.* **106**, 18054 (2009).
4. B. A. Halkier, J. Gershenzon, *Annu. Rev. Plant Biol.* **57**, 303 (2006).
5. R. J. Hopkins, N. M. van Dam, J. J. A. van Loon, *Annu. Rev. Entomol.* **54**, 57 (2009).
6. G. Brader, M. D. Mikkelsen, B. A. Halkier, E. Tapio Palva, *Plant J.* **46**, 758 (2006).
7. M. Bressan *et al.*, *ISME J.* **3**, 1243 (2009).
8. C. A. Rushworth, B. H. Song, C.-R. Lee, T. Mitchell-Olds, *Mol. Ecol.* **20**, 4843 (2011).
9. A. Brunelle, C. Whitlock, P. Bartlein, K. Kipfmueller, *Quat. Sci. Rev.* **24**, 2281 (2005).
10. M. E. Schranz, A. J. Manzaneda, A. J. Windsor, M. J. Clauss, T. Mitchell-Olds, *Heredity* **102**, 465 (2009).
11. A. J. Windsor *et al.*, *Phytochemistry* **66**, 1321 (2005).
12. See supplementary materials on *Science* Online.
13. M. E. Schranz, A. J. Windsor, B. H. Song, A. Lawton-Rauh, T. Mitchell-Olds, *Plant Physiol.* **144**, 286 (2007).
14. B. Reintanz *et al.*, *Plant Cell* **13**, 351 (2001).
15. S. X. Chen *et al.*, *Plant J.* **33**, 923 (2003).
16. S. Bak, F. E. Tax, K. A. Feldmann, D. W. Galbraith, R. Feyereisen, *Plant Cell* **13**, 101 (2001).
17. P. Naur *et al.*, *Plant Physiol.* **133**, 63 (2003).
18. Z. Yang, *Mol. Biol. Evol.* **24**, 1586 (2007).
19. T. L. Poulos, E. F. Johnson, in *Cytochrome P450: Structure, Mechanism, and Biochemistry*, P. R. Ortiz de Montellano, Ed. (Kluwer Academic/Plenum, New York, 2005), pp. 217–271.
20. T. L. Poulos, Y. T. Meharenna, in *The Ubiquitous Roles of Cytochrome P450 Proteins*, A. Sigel, H. Sigel, R. K. O. Sigel, Eds. (Wiley, Chichester, UK, 2007), pp. 57–96.

Acknowledgments: We thank R. Colautti, K. Donohue, M. Feder, T. Pendergast, M. Rausher, C. Rushworth, A. Shumate, M. Wagner, J. Willis, and two anonymous reviewers for helpful comments. K. Springer, E. Ballweg, M. Cameron, K. Chu, S. Hurst, V. Cousins, K. Dales, R. Doll, J. Lutkenhaus, M. Mitchell-Olds, S. Mitchell-Olds, E. Raskin, J. Rivera, L. Saucier, M. Wagner, and T. Weiss-Lehman helped in lab and field. N. Wicks and Bitterroot National Forest allowed us to work on their property. We thank the Heald family for support and hospitality. Supported by NIH grants R01-GM086496 (T.M.-O.) and R01-GM079530 (M.A.S.), NSF grant EF-0723447 (T.M.-O.); NSF dissertation grants 1011167 (C.O.-M.) and 1110445 (C.-R.L.); and a Netherlands Organization for Scientific Research (NWO) Ecogenomics grant (M.E.S.). Data in the supplementary materials are also available as GenBank accession nos. JX185680, JX185681, and BCMA JQ337904 to BCMA JQ337909. Data are deposited in the Dryad Repository: http://dx.doi.org/10.5061/dryad.kc6m8.

Supplementary Materials

www.sciencemag.org/cgi/content/full/337/6098/1081/DC1
Materials and Methods
Supplementary Text
Figs. S1 to S8
Tables S1 to S20
References (*21*–*55*)

8 March 2012; accepted 19 June 2012
10.1126/science.1221636

Arbuscular Mycorrhizal Fungi Increase Organic Carbon Decomposition Under Elevated CO_2

Lei Cheng,[1]* Fitzgerald L. Booker,[2,3] Cong Tu,[1] Kent O. Burkey,[2,3] Lishi Zhou,[1,4] H. David Shew,[1] Thomas W. Rufty,[3] Shuijin Hu[1]†

The extent to which terrestrial ecosystems can sequester carbon to mitigate climate change is a matter of debate. The stimulation of arbuscular mycorrhizal fungi (AMF) by elevated atmospheric carbon dioxide (CO_2) has been assumed to be a major mechanism facilitating soil carbon sequestration by increasing carbon inputs to soil and by protecting organic carbon from decomposition via aggregation. We present evidence from four independent microcosm and field experiments demonstrating that CO_2 enhancement of AMF results in considerable soil carbon losses. Our findings challenge the assumption that AMF protect against degradation of organic carbon in soil and raise questions about the current prediction of terrestrial ecosystem carbon balance under future climate-change scenarios.

Arbuscular mycorrhizal fungi (AMF), which form associations with roots of ~80% of land plant species, obtain carbon (C) from their host plants in return for mineral nutrients (*1*, *2*). AMF utilize a large proportion (up to 20%) of net plant photosynthates under ambient atmospheric CO_2 (aCO_2) (*3*, *4*), deposit slow cycling organic compounds such as chitin and glomalin (*1*, *5*), and protect organic matter from microbial attack by promoting soil aggregation (*6*). AMF thus play a critical role in the global C cycle. Atmospheric CO_2 enrichment often increases plant photosynthate allocation to AMF and stimulates the growth of AMF (*3*, *7*–*9*), leading to a proposition that global soils may sequester more C through mycorrhizal symbioses under future scenarios of elevated CO_2 (eCO_2) (*3*, *5*, *7*–*12*). This hypothesis, however, does not consider the effect of AMF on decomposition under eCO_2. Indeed, AMF growth can result in enhanced decomposition of complex organic material and alter plant N uptake (*13*–*15*).

We conducted four independent but complementary experiments to investigate how CO_2 stimulation of AMF affects organic C decomposition in soil and the subsequent N dynamics in the plant-soil system by combining dual $^{13}C/^{15}N$ labeling and hyphae-ingrowth techniques (*16*). We first ascertained the effect of eCO_2 [main plot, $n = 4$; ambient at 380 versus elevated at 580 parts per million by volume (ppmv)] and N addition (subplot; control at 0 versus added at 5 g N m^{-2}) on

[1]Department of Plant Pathology, North Carolina State University, Raleigh, NC 27695, USA. [2]United States Department of Agriculture, Agricultural Research Service, Plant Science Research Unit, Raleigh, NC 27607, USA. [3]Department of Crop Science, North Carolina State University, Raleigh, NC 27695, USA. [4]State Key Laboratory of Vegetation and Environmental Change, Institute of Botany, Chinese Academy of Sciences, Xiangshan, Beijing 100093, China.

*Present address: Department of Ecosystem Science and Management, The Pennsylvania State University, University Park, PA 16802, USA.

†To whom correspondence should be addressed. E-mail: shuijin_hu@ncsu.edu